2023 IEEE Energy Conversion Congress and Exposition (ECCE) | 979-8-3503-1644-5/23/$31.00 ©2023 IEEE | DOI: 10.1109/ECCE53617.2023.10362174

The Analysis, Design, and Optimization of an Electronic MOV Circuit for the Solid-State Circuit Breaker Applications

Yuntao Xu, Di Zhang and Brandon Keck
Department of Electrical and Computer Engineering
Naval Postgraduate School
Monterey, USA
yuntao.xu@nps.edu, di.zhang@nps.edu, brandon.keck@nps.edu

Lakshmi Ravi
Bradley Department of Electrical and Computer Engineering
Vrignia Tech
Blacksburg, USA
lravi@vt.edu

Zheyu Zhang and Dehao Qin
College of Engineering, Computing and Applied Sciences
Clemson University
Charleston, USA
zheyuz@clemson.edu, dehaoq@g.clemson.edu

***Abstract*— The electronic metal oxide varistor (eMOV) is the series connection of a traditional MOV and a thyristor with its gate controlled by a breakover diode (BOD). Compared with the traditional solid-state circuit breaker (SSCB) design, the eMOV allows the decoupling of the MOV clamping voltage and the direct current (DC) system voltage and proves essential for efficiency and power density enhancement. This paper focuses on the operation details and optimization of the eMOV. In-depth analysis and experimental results are provided to validate the eMOV design methodology and highlight the key application aspects.**

Keywords—solid state circuit breaker, hybrid electric propulsion, protection, MOV, breakover diode

I. INTRODUCTION

Electrified aircraft propulsion is a promising trend for future aviation applications. To reduce the weight of the electric power system, the medium-voltage direct current (MVDC) system is preferred. As a protection device to handle the system short circuit fault, compared with the mechanical breaker and hybrid circuit breaker, the solid-state circuit breaker (SSCB) is advantageous due to its ultrafast response, arc free operation and simple structure [1]. As the solid-state devices employed in the SSCB, such as the silicon (Si) insulated gate bipolar transistor (IGBT), are limited in both their surge-energy capability and the available breakdown voltage rating, a voltage clamping and energy absorbing circuit is often used in parallel with the solid-state branch, traditionally composed of metal-oxide varistors (MOVs). The large separation between the MOV's clamping voltage and its continuous DC voltage rating negatively impacts the weight, size, and efficiency of the SSCB.

To solve this issue, an electronic MOV (eMOV) was proposed in [2] which consists of a traditional MOV in series with a thyristor (SCR) with its gate controlled by a breakover diode (BOD). This configuration allows the decoupling of the MOV's clamping voltage and SSCB's nominal working voltage, resulting in a more compact and efficient SSCB design. The eMOV working principle and component selection criteria were covered in [2]. However, the detailed component optimization, especially the impact of component parasitics, and the full power experimental results were not included. This paper continues to focus on the design aspects and optimization of the eMOV based on extensive experimental data, aiming at a deeper understanding and a design methodology fully supported by detailed analysis.

This paper is organized as follows: Section II reviews the working principle of the eMOV and its operational advantages over the traditional voltage clamping circuit (VCC). In section III, equivalent circuit models at different operating stages of the SSCB are established to account for those aspects relevant to eMOV design optimization and to facilitate qualitative and, where applicable, quantitative analysis of eMOV operation. Experimental results are presented in Section IV to verify the analysis, followed by conclusions in Section V.

II. REVIEW OF OPERATION PRINCIPLE OF THE eMOV

An SSCB is solely based on power semiconductor devices, with no mechanical switch or moving parts. A typical IGBT-based SSCB capable of current flow and voltage blocking in both directions (i.e., four-quadrant operation) is shown in Fig. 1. It consists of two IGBT modules connected in anti-series and a voltage clamping device. Each IGBT module incorporates an antiparallel diode to allow bidirectional current flow. The anti-series connection of two IGBT modules realizes voltage blocking capability in both polarities. The VCC is connected in parallel with the semiconductor modules to provide a current commutation path and voltage containment during the opening, or turn-off, of the SSCB. In high power applications, the VCC is usually implemented with a metal oxide varistor (MOV) due to its highly nonlinear voltage-current characteristics and high energy absorption capability, as shown in Fig. 2(a).

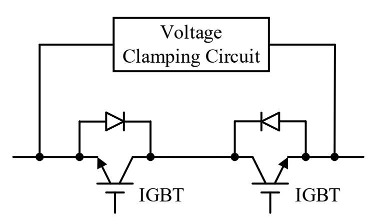

Fig. 1: Topology of a typical IGBT-based SSCB.

Authorized licensed use limited to: UNIVERSITY OF TENNESSEE LIBRARIES. Downloaded on April 19,2024 at 12:54:04 UTC from IEEE Xplore. Restrictions apply.

The MOV has highly nonlinear *V-I* characteristics, and three distinct regions of electrical operation can be identified, i.e., leakage region, normal varistor region or clamping region, and upturn region [3]. In the traditional MOV-based VCC shown in Fig. 2(a), when the SSCB is in open state, the MOV is subjected to the DC system voltage V_{dc}. For the standby dissipation to stay below its continuous power rating, the MOV rated DC voltage $V_{M(DC)}$ must be higher than V_{dc}. During the SSCB turn-off transient, the DC system current I_{dc} is commutated to the MOV. The MOV enters the clamping region and its characteristic in this region determines the peak voltage V_{pk} across the IGBT module. For a typical MOV, there exists significant separation between its rated DC voltage and the clamping voltage. For example, V511DB40 by Littelfuse has a rated DC voltage $V_{M(DC)}$ of 675 V, and its clamping voltage V_C is 1350 V at a 200 A 8/20 µs current pulse. For an SSCB, the current pulse can be significantly higher and so will the clamping voltage. Such wide separation between voltage $V_{M(DC)}$ and V_C necessitates the use of IGBTs with a voltage rating higher than what is typical for a given DC system voltage, resulting in an SSCB with higher weight and larger size, more dissipation during conduction, and reduced efficiency.

To circumvent the limitation posed by the traditional MOV-based VCC, an auxiliary switch can be added as shown in Fig. 2(b). The auxiliary switch stays open when the SSCB is off, separating the voltage across the MOV during standby from the DC system voltage V_{dc}. During the SSCB turn-off transient, the auxiliary switch is closed and the MOV clamps the voltage across the IGBT modules. With this arrangement, the MOV can be selected based on the desired clamping voltage rather than its rated DC voltage. A most economic SSCB design can be achieved with this new freedom.

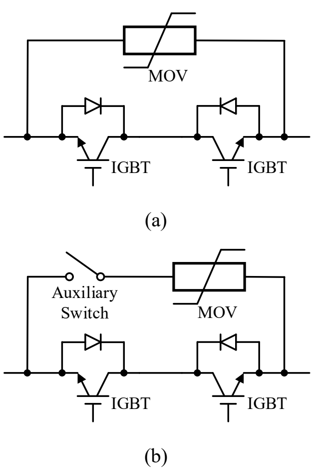

Fig. 2: VCC implemented with MOV. (a) Tranditional implementation. (b) Use of an auxliary switch to decouple the DC system voltage from its standby voltage.

The auxiliary switch shown in Fig. 2(b) should automatically engage during the SSCB turn-off transient, and it should be implemented with fast solid-state devices to facilitate timely current commutation and voltage clamping. After the turn-off transient, the auxiliary switch should automatically return to the open state and decouple the MOV from the DC source voltage. A thyristor with a BOD connected between its anode and gate, as shown in Fig. 3, implements the auxiliary switch satisfying the requirements stipulated above. The resulting VCC is termed the eMOV [2], since the MOV is electronically connected across the IGBT modules to clamp the voltage when called for. It is noted that such automatic turn-on of the thyristor when its terminal voltage exceeds certain limit for overvoltage protection is well known [4], [5]. However, its deployment in the SSCB is novel, and the design aspects unique to the SSCB application need to be considered. The antiparallel connection of the two identical BOD-driven thyristor branches accommodates the bidirectional SSCB operation. Components across the gate and cathode of the SCR help to prevent parasitic triggering. The reverse blocking diode in series with the BOD is needed since the BOD has limited reverse blocking capability. The resistor in series with the reverse blocking diode limits the current upon BOD breakover. R_{a1} or R_{a2}, and R_b, resistors of high resistance and in parallel with the BOD and the MOV, respectively, form a voltage divider to achieve a well-defined standby voltage across the MOV.

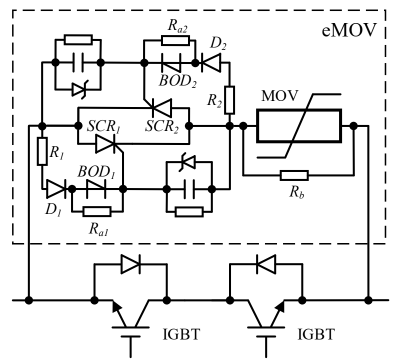

Fig. 3: SSCB Schemmatic with the eMOV.

The working principle of the eMOV during SSCB turn-off is detailed in [2] and outlined in Fig. 4 for reference. The RC snubber is added to alleviate the switching stress incurred in the IGBT and to reduce *dv/dt* during turn-off. R_{a1} and R_b are irrelevant during turn-off and are omitted to reduce the crowdedness in these circuit diagrams.

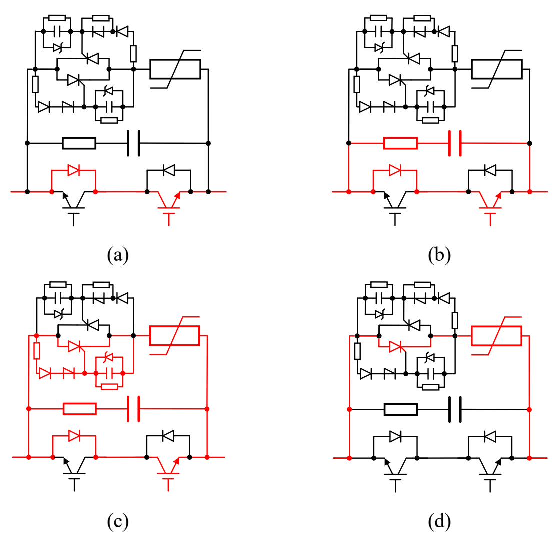

Fig. 4: Major operation stages during SSCB turn-off: (a) Prior to turn-off. (b) IGBT turn-off initiated. (c) eMOV enaged. (d) System current decay

Authorized licensed use limited to: UNIVERSITY OF TENNESSEE LIBRARIES. Downloaded on April 19,2024 at 12:54:04 UTC from IEEE Xplore. Restrictions apply.

III. Circuit Models and Analysis of the eMOV

The eMOV has distinctive operating modes depending on the SSCB status. To better elucidate the eMOV operation details and identify the design aspects key to its performance, equivalent circuits are established to facilitate detailed analysis and performance prediction. The analysis results help to explain and understand the experimental data and to optimize the components for eMOV implementation.

Referring to Fig. 3 and Fig. 4, the following operating modes can be identified:

1. When the SSCB is open (i.e., IGBTs are off), the DC source voltage is divided between the MOV and SCR per the resistance values in the voltage divider consisting of R_a and R_b.

2. When the IGBTs are turned on, the voltage across the eMOV collapses. The MOV and SCR voltages drop at rates determined by parasitic capacitances, ending up with positive and negative polarities, respectively. Afterwards, both the MOV and SCR voltages decay to close to zero, with the decaying rate determined by the parasitic capacitances and resistors.

3. When the IGBTs are turned off to open the SSCB, the MOV and SCR voltages rise at rates determined by parasitic capacitances. The SCR turns on after the BOD breaks over, and the MOV clamps the voltage across the SSCB.

4. After the IGBT turn-off, the system current, due to load or fault, flows through the MOV, decaying at a rate determined by the DC source voltage, the MOV clamping characteristic, and the system inductance. The circuit energy is absorbed by the MOV. The SCR turns off after the MOV current decays below the SCR holding current and the system current is cleared. The voltage distribution between the MOV and SCR is restored to that prior to the IGBT turn-on.

In the following, the equivalent circuit for each mode is presented and analyzed.

A. SSCB Standby

During standby with IGBTs off, the DC source voltage appears across the eMOV and is divided between the MOV and SCR sections, as shown in Fig. 5, where R_a corresponds to either R_{a1} or R_{a2}, depending on the DC source voltage polarity. Without a dedicated voltage divider consisting of R_a and R_b, the voltage division would be determined by the leakage characteristics of the MOV, SCR and BOD. To eliminate the dependence on the component leakage impedances and to guarantee that a desired portion of the DC source voltage appears across the MOV, the resistances of R_a and R_b should be sufficiently high to minimize dissipation while much lower than the component leakage impedances. If R_a and R_b are of the same resistance, the MOV standby voltage is half of the DC source voltage.

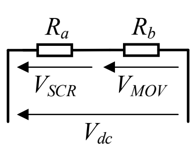

Fig. 5: Equivalent circuit during standby

B. SSCB Turn-on Transient

Upon IGBT turn-on, the voltage across the eMOV collapses. Consequently, the parasitic capacitances of the eMOV components, including the MOV, SCRs, BODs and reverse blocking diodes, discharge through the IGBT modules. The equivalent circuit shown in Fig. 6 depicts this scenario, where the SCR section capacitance is a composite accounting for the capacitance of any reverse-biased PN junction present in the SCRs, BODs or reverse blocking diodes. All these capacitances are voltage dependent and nonlinear. The component datasheet does not always provide sufficient capacitance information, and special measurement or experiment needs to be conducted to obtain such information.

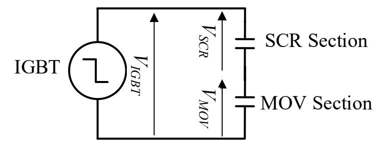

Fig. 6: Simplified eMOV equivalent circuit during SSCB turn-on transient.

For detailed analysis of the eMOV response during the SSCB switching transient, the composite capacitance of the SCR section can be expanded as shown in Fig. 7. The correspondence between the capacitances in Fig. 7 and the actual components shown Fig. 3 can be easily identified. Those components irrelevant to the transient analysis, such as the voltage divider and the filtering and protection circuit between the SCR gate and cathode, are omitted from the equivalent circuit. The SCR and BOD are four-layer devices with three PN junctions, and the bias status of these junctions is dependent on the circuit operating condition. The capacitance representing the reverse blocking diode reduces to a short when it becomes forward biased. Therefore, the circuit configuration as well as component parameter can change during the switching transient, for example due to the breakover of a BOD or when a reverse blocking diode changes from reverse biased to forward biased.

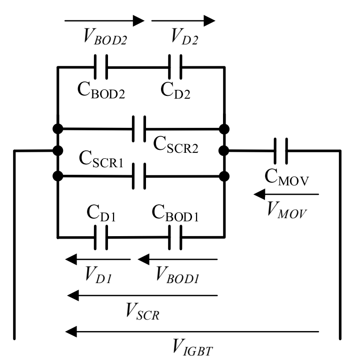

Fig. 7: Detailed eMOV equivalent circuit during SSCB swtitching transient.

During the SSCB turn-on transient with V_{IGBT} collapsing from the DC source voltage towards zero, the capacitances shown in Fig. 7 determine the discharge rate and transient voltage profile of each component. For example, if the composite capacitance of the SCR section is much lower than the MOV capacitance, the majority of the transient voltage occurs across the SCR section. Similarly, inside each BOD

Authorized licensed use limited to: UNIVERSITY OF TENNESSEE LIBRARIES. Downloaded on April 19,2024 at 12:54:04 UTC from IEEE Xplore. Restrictions apply.

branch of the SCR section, the shares of the SCR section transient voltage assumed by the BOD and the reverse blocking diode are determined by their capacitances. The voltage experienced by each component could trigger sudden behavior change, affecting the circuit transient. For example, the BOD will break over when its terminal voltage exceeds its breakover rating, and the SCR or the BOD could be switched on due to high *dv/dt* across its anode and cathode.

C. SSCB Turn-off Transient

Upon IGBT turn-off, the voltage across the eMOV increases. Consequently, the parasitic capacitances of the eMOV components are charged up. A simplified equivalent circuit similar to Fig. 6 is shown in Fig. 8 to represent this scenario. The detailed eMOV equivalent circuit shown in Fig. 7 still applies for the analysis of its behavior during the turn-off transient.

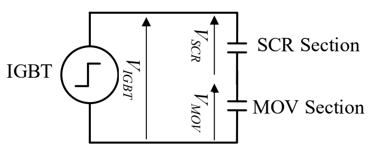

Fig. 8: Simplified equivalent circuit during SSCB turn-off transient.

Since voltage clamping and energy absorption are the primary reasons for its deployment, the eMOV behavior during the SSCB turn-off transient is critical. It is desirable for the SCR section to switch on and engage the MOV as soon as possible. This suggests that most of the transient voltage should appear across the SCR section. Accordingly, it is advantageous to have the MOV section capacitance dominate that of the SCR section. This can be achieved by connecting a high voltage ceramic capacitor in parallel with the MOV.

D. Energy Absorption and Current Clearing

With the IGBT turned off and all the current commutated to the eMOV branch, the system current decays at a rate determined by the MOV characteristics, the circuit inductance, as well as the source and load condition. Fig. 9 shows the equivalent circuit in the case of clearing a dead short, where L_{System} represents the inductance due to the source impedance as well as the cabling and any inductive component such as a current limiting inductor.

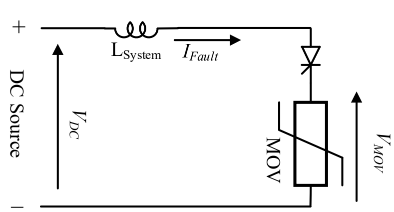

Fig. 9: Equivalent circuit showing energy absorption and current clearing in the case of dead short.

After the system current decays below the SCR holding current, the SCR turns off. At this point, the SSCB terminal voltage is not necessarily equal to the DC source voltage. If an RC snubber is used in parallel with the eMOV as shown in Fig. 4, another transient will ensue which involves the system inductance and the RC snubber and gradually brings the SSCB terminal voltage to the DC source voltage.

The MOV leakage current at the DC source voltage should be lower than the SCR holding current to guarantee that the SCR can turn off. The SCR does not restore its voltage blocking capability right after it turns off. In the typical eMOV configuration, usually there is insufficient current flow in the negative direction for quick sweep-out of the stored charge in the SCR, and the internal recombination would be major mechanism for charge removal. This results in a turn-off time much longer than that listed in the SCR datasheet.

IV. Prototyping and Experimentation

A 2 kV 1.2 kA SSCB prototype with an eMOV integrated is built, as shown in Fig. 10. Extensive switching test has been conducted to evaluate and optimize its performance. The circuit diagram of the test bed is shown in Fig. 11, where the SSCB schematic is detailed as well. The SSCB consists of two IGBT modules (FZ3300R33HL3) connected back-to-back, an RC snubber (R_S = 0.47 Ω and C_S = 1.5 µF), and an eMOV with the components listed in Table I. It is worth noting that this SSCB features an inductor-less design, where no current limiting inductor is used and the fault current limiting is achieved with the use of reduced on-state gate voltage [6]. A capacitor bank emulates the DC source and an air-core inductor represents the system inductance, which is adjustable between 0-50µH. The function generator issues the switching command to the SSCB. The transient voltage and current waveforms are captured using an 8-channel oscilloscope (Tektronix MSO58 5−BW−350).

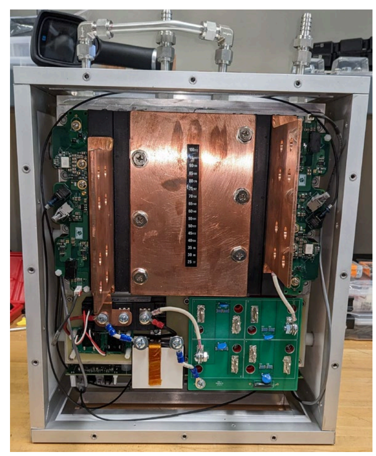

(a)

(b)

Fig. 10: Photos of the 2 kV 1.2 kA SSCB prototype. (a) Fully packaged SSCB. (b) Zoom-in view of the eMOV.

Authorized licensed use limited to: UNIVERSITY OF TENNESSEE LIBRARIES. Downloaded on April 19,2024 at 12:54:04 UTC from IEEE Xplore. Restrictions apply.

The SSCB is capable of four-quadrant operation. The test configuration shown in Fig. 11 focuses on its behavior in one quadrant only. The results, however, are general and applicable under other operating conditions due to its symmetric topology. In this configuration, the lower IGBT actively participates in the switching while the freewheel diode of upper IGBT module completes the current path. In the SCR section of the eMOV, the branch consisting of SCR_1 and BOD_1 acts to engage the MOV during SSCB turn-off, while the antiparallel branch consisting of SCR_2 and BOD_2 is not expected to act. An extra capacitance, C_b, is shown in parallel with the MOV, representing external capacitance to reduce the share of transient voltage across the MOV and expedite the BOD breakover.

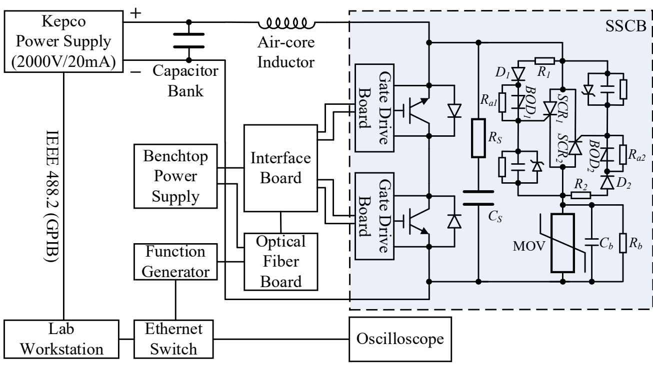

Fig. 11: Circuit diagram of the switching test bed.

TABLE I. LIST OF eMOV COMPONENTS AND/OR PARAMETERS

MOV, 2 in Parallel, 2 in Series	V511DB40
SCR Module	MCC200-18IO1
BOD	IXBOD01-06
Reverse Blocking Diode	GD25MPS17H
Current Limiting Resistor	10 Ω
Filter Between SCR Gate and Cathode	10 Ω,18 nF, Zener (8.2 V)
High Voltage Resistors R_{a1}, R_{a2} and R_b	6 MΩ
Additional Capacitor Across Each MOV	3300 pF

A. *SSCB Switching Transient Test Resuslts*

Fig. 12 and Fig. 13 present the SSCB voltage and current waveforms during the interruption of a short circuit developed at a DC source voltage of 2000 V with the system inductance L_{System} equal to 25 µH and less than 0.5 µH, respectively. The short circuit is detected by the gate drive's desaturation protection circuit and then the SSCB opening is initiated. With L_{System} equal to 25 µH, the fault current is interrupted before the IGBT enters the active region. With L_{System} less than 0.5 µH, the IGBT enters the current saturation mode before the fault is detected by the protection circuit thanks to the reduced gate voltage, achieving fault current limiting in spite of the lack of a current limiting inductor. In both cases, the IGBT voltage and current trajectories during the short circuit current interruption stay well within its reverse bias safe operating area, due to the properly designed eMOV as well as the RC snubber.

In these waveforms, the four operating modes as detailed in III can be easily identified. When the SSCB is off, the DC source voltage is equally shared by the SCR section and the MOV with R_{a1}, R_{a2} and R_b of the same resistance. When the IGBTs are gated on to close the SSCB, the IGBT voltage collapses, and the SCR section and MOV discharge at different rates. When the IGBTs are commanded to open by the protection circuit, the IGBT voltage rises, and the SCR section and MOV are charged up at different rates. This lasts until the BOD breaks over, resulting in the commutation of the system current to the MOV. The MOV provides voltage clamping and absorbs the inductive energy in the circuit. The SCR turns off after the current decays below its holding current. The SCR eventually starts to assume voltage, after several to tens of milliseconds, not shown here due to the long time window required to capture this process.

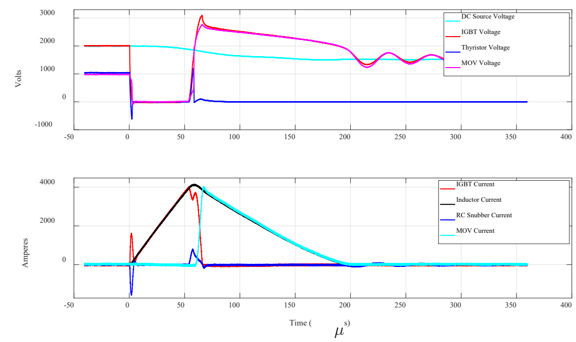

Fig. 12: SSCB switching waveforms, L_{System} = 25µH, V_{DC} = 2000V.

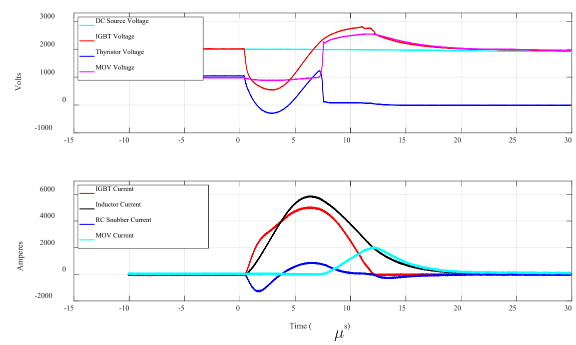

Fig. 13: SSCB switching waveforms, $L_{System} \leq$ 0.5µH, V_{DC} = 2000V.

Close inspection of the waveforms does expose interesting aspects of the eMOV behavior worth further investigation, as detailed in the following subsections.

B. *Detailed eMOV Behavior During SSCB Turn-on Transient*

Fig. 14 zooms in on the voltage waveforms around the SSCB turn-on event. For comparison, the case where the DC source voltage is 1200 V is also shown. In both cases, the SCR section discharges much faster than the MOV section, resulting in polarity reversal of V_{SCR}. In the case where V_{DC} = 2000 V, V_{SCR} collapses after V_{SCR} approaches about -600 V. By contrast, in the case where V_{DC} = 1200 V, V_{SCR} and V_{MOV} settle down at voltages of equal magnitude and opposite polarities. Referring to Fig. 7, when V_{SCR} turns negative, SCR_2 and BOD_2 in the antiparallel branch become forward biased. Both of them could potentially be turned on by high *dv/dt*. Inspection of V_{SCR} , though, does not indicate that *dv/dt* is approaching the datasheet value of 1000 V/µs. In the meantime, V_{SCR} still is far from -1200 V, the BOD breakover voltage, and it is not apparent that BOD_2 would act. To explain the eMOV behavior, it is necessary to inspect V_{BOD2} during the transient.

Authorized licensed use limited to: UNIVERSITY OF TENNESSEE LIBRARIES. Downloaded on April 19,2024 at 12:54:04 UTC from IEEE Xplore. Restrictions apply.

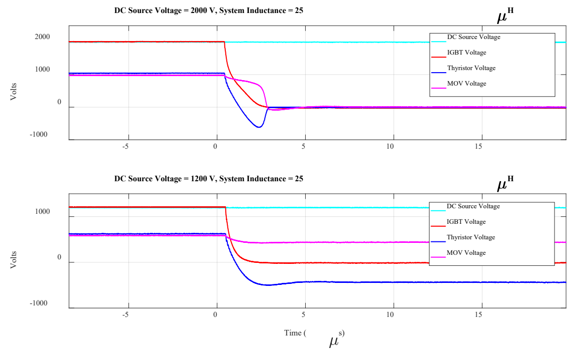

Fig. 14: Zoom-in view of the voltage waveforms during the SSCB turn-on transient at different DC source voltages.

Fig. 15 presents the transient voltages across the components inside the eMOV. V_{BOD1}, V_{BOD2} and V_{D2} denote voltages across BOD_1, BOD_2 and D_2 , respectively, measured from the anode to cathode. It is noticed most of the transient change in V_{SCR} is assumed by the BOD. This can be attributed to the fact that the BOD capacitance C_{BOD} much lower than the reverse blocking diode capacitance C_D. In the case where V_{DC} = 2000 V, V_{BOD2} rises above 1200 V and BOD_2 breaks over. Following this, the D_2 junction capacitance quickly discharges and D_2 becomes forward biased. The other junction capacitances in the SCR section, C_{SCR1}, C_{SCR2}, C_{BOD1} and C_{D2}, continue to discharge through the BOD_2 branch. The MOV capacitance replenishes the charge until BOD_2 fully turns on and quickly discharges all the capacitances in the eMOV. This transient process can be further confirmed by the waveforms shown in Fig. 16, where the current flowing from BOD_2 to the gate of SCR_2 is displayed. In the case where V_{DC} = 1200 V, V_{BOD2} does not rise to the breakover point, and no such transient occurs. Instead, the voltages across the SCR and MOV sections and those across BOD_1, BOD_2, D_1 and D_2 slowly decay toward zero, with time constants up to tens of milliseconds as determined by the component parasitic capacitances, leakage characteristics and . R_{a1} or R_{a2}, and R_b. In the switching test setup shown in Fig. 11, the on-time of the SSCB usually does not exceed tens of microseconds. Therefore, the steady state voltage redistribution after the turn-on is not visible.

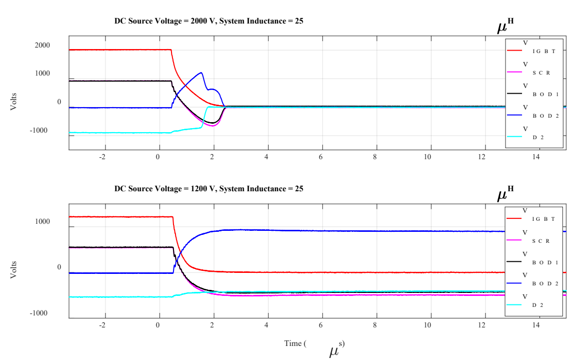

Fig. 15: eMOV component voltage waveforms during the SSCB turn-on transient at different DC source voltages.

Note that the breakover of the BOD as described above during the SSCR turn-on transient does not affect the SSCB operation. It does not result in turn-on of the SCR since the external circuit does not provide sufficient current to hold or even latch the SCR in the on state. The momentary breakover of the BOD actually expedites the voltage distribution towards the steady state, albeit not intended.

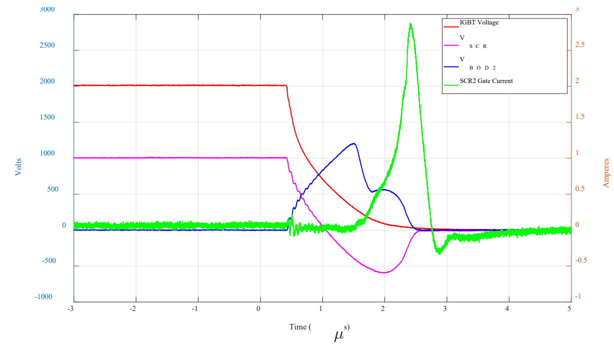

Fig. 16: Transient voltage and current waveforms in the BOD2 branch during the SSCB turn-on transient at different DC source voltages.

C. Detailed eMOV Behavior During SSCB Turn-off Transient

As discussed in III.C, it is desirable to have the SCR section to assume the majority of the transient IGBT voltage rise during turn-off, so that the BOD can break over and turn on the SCR, engaging the MOV for voltage clamping as soon as possible. The external ceramic capacitor C_b across the MOV, as shown in Fig. 11, is installed for this purpose. Fig. 17 compares the waveforms before and after the adding of external capacitance, under the otherwise identical test conditions. The increased BOD voltage ramp rate, quicker engagement of the MOV and reduced IGBT peak voltage are apparent.

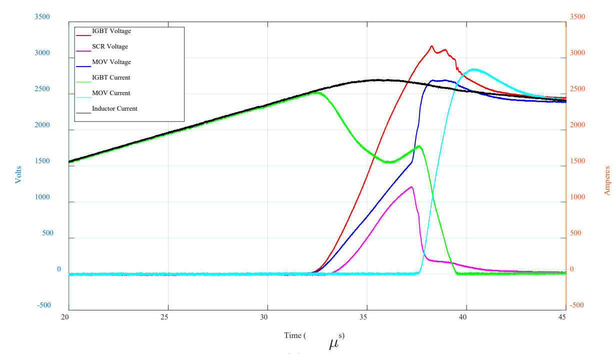

(a)

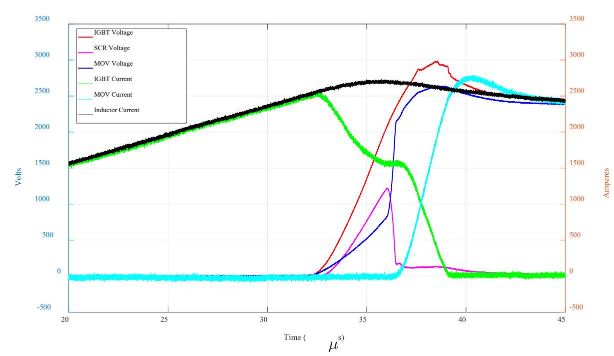

(b)

Fig. 17: Comparison of the waveforms during IGBT turn-off. (a) Default configuration without the external capacitor across the MOV. (b). With the external capacitor installed across the MOV.

Authorized licensed use limited to: UNIVERSITY OF TENNESSEE LIBRARIES. Downloaded on April 19,2024 at 12:54:04 UTC from IEEE Xplore. Restrictions apply.

D. Packaging and Physical Connection of the eMOV

The physical connection of the eMOV components has an impact on its performance. It is obvious that the eMOV should be packaged as close to the IGBT modules as possible to minimize the commutation loop inductance. The high *di/dt* induced voltage during commutation adds to the MOV clamping voltage and increases the IGBT peak voltage stress.

Hardware photos in Fig. 10 show the packaged SSCB and the way eMOV is incorporated. The small PCB right next to the SCR module is where smaller components shown in blue in Fig. 18(a) are installed and is called the trigger PCB. This PCB, shown in Fig 18(b) and Fig 18(c), has two ports, P1 and P2, feeding the gates of the two SCRs. The other two larger connection points, A1-K2 and K1-A2, are intended for connection to the SCR module power terminals. Fig. 19 depicts the wiring between the components inside the SSCB, where the copper wires and buses are shown in golden color with the line thickness indicating the conductor size.

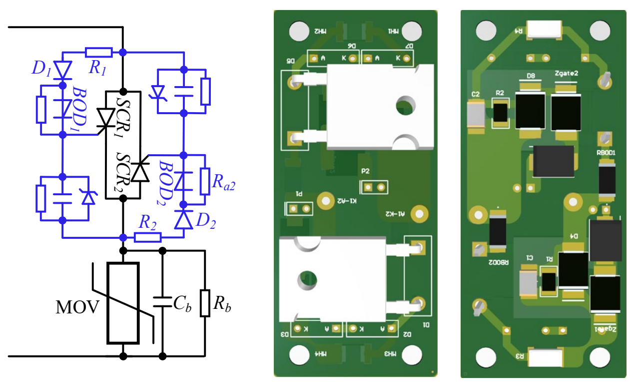

(a) (b) (c)

Fig. 18: Small PCB in eMOV. (a) Componenets installed on PCB shown in blue. (b). Top side of PCB. (c). Bottom side of PCB.

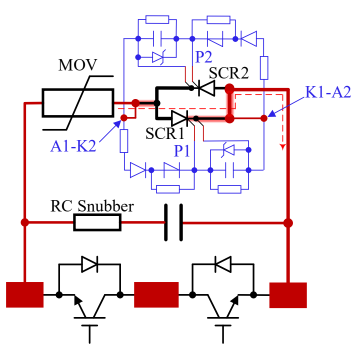

Fig. 19: Components wiring inside the SSCB.

It is noticed that with the trigger PCB connected as shown, unintended current circulation loops would arise. For example, P2/K, the auxiliary cathode connection in port P2, and A1-K2 would form a loop when they are simultaneously connected to the SCR module. Such a loop will see significant current flow when the fault/load current is commutated to the eMOV at high *di/dt*. For example, the dashed line in Fig. 19 indicates the current flow direction after SCR_1 is turned on. The black lines with a glow indicate copper buses inside the SCR module where voltage is induced due to *di/dt*. This voltage would drive current in the unintended loop where the only impedance is the loop inductance and resistance. To avoid this, only ports P1 and P2 should be connected to the SCR module. Fig. 20 shows the current flow in the P2/K connection wire from the SCR to the trigger PCB around the BOD breakover, with and without A1-K2 connected to the SCR module, respectively. The BOD breakover results in the sharp current pulse entering the SCR_1 gate, turning on SCR_1 and initiating current commutation. As shown in the top graph of Fig. 20, the *di/dt* induced voltage leads to circulating current above 100 A in the SCR_2 cathode loop when A1-K2 is connected to the SCR power terminal. Without the A1-K2 connection, the current in the P2/K connection wire returns to normal as shown in the lower graph. The *di/dt* induced voltage also causes the additional gate current bump after the sharp pulse, and a notch in it.

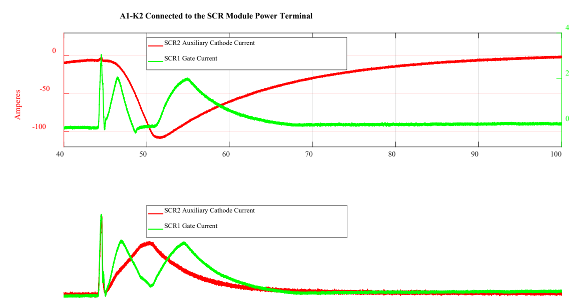

Fig. 20: Current flow in P2/K connections with and without A1-K2 connected to the SCR module.

V. Conclusion

As a key part of a compact SSCB for MVDC applications [6], the eMOV combines the conventional MOV with a pair of BOD-triggered SCRs to decouple the MOV's clamping voltage and the DC source voltage. This paper performs an in-depth study of the eMOV behavior observed in an SSCB prototype. Circuit models are developed for detailed analysis of the eMOV transient operating modes. The design and application aspects for the optimization of the eMOV are presented.

References

[1] R. Rodrigues, Y. Du, A. Antoniazzi and P. Cairoli "A Review of Solid-State Circuit Breakers," in IEEE Transactions on Power Electronics, vol. 36, no. 1, pp. 364-377, Jan. 2021.

[2] L. Ravi, D. Zhang, D. Qin, Z. Zhang, Y. Xu and D. Dong, "Electronic MOV-Based Voltage Clamping Circuit for DC Solid-State Circuit Breaker Applications," in IEEE Transactions on Power Electronics, vol. 37, no. 7, pp. 7561-7565, July 2022.

[3] Littelfuse, Appl. Note 9767.1, Littelfuse Varistors - Basic Properties, Terminology and Theory, July 1999.

[4] H. M. Lawatsch and J. Vitins, "Protection of thyristors against overvoltage with breakover diodes," in IEEE Transactions on Industry Applications, vol. 24, no. 3, pp. 444-448, May-June 1988.

[5] Littelfuse, Appl. Note, High Power Semiconductor Crowbar Protector for AC Power Line Applications, 2020.

[6] D. Zhang, Y. Xu, J. Brandt, Z. Zhang, D. Qin and D. Dong, "A Solid-State Circuit Breaker Without Current Limiting Inductor," in IEEE Transactions on Industry Applications, vol. 59, no. 4, pp. 4640-4650, July-Aug. 2023.

Authorized licensed use limited to: UNIVERSITY OF TENNESSEE LIBRARIES. Downloaded on April 19,2024 at 12:54:04 UTC from IEEE Xplore. Restrictions apply.